

Magnetic footprints in the DIII-D USN with C-Coils like configuration using method of maps

Halima Ali¹, Alkesh Punjabi¹, Allen Boozer², and Todd Evans³

¹*Center for Fusion Research & Training, Hampton University, Hampton, VA 23668 USA*

²*Columbia University, New York, New York 10027, USA*

³*General Atomics, San Diego, California 92186, USA*

ABSTRACT: The DIII-D tokamak with upper single-null, ELMs, and C-coils like configuration is simulated using method of maps [1,2]. When the ELMs and C-coils are off, the footprint consists of six strips running toroidally. The key effect of the ELMs is that it organizes the footprint into a single large-scale, large-size coherent structure. Turning on the C-coils forces this structure to first bifurcate into two toroidal strips, and then to trifurcate into three toroidal strips. Taking the width of the stochastic layer and the area of the footprint with ELMs on as the base, the width of stochastic layer scales as $I_{c-coils}^{0.4}$, while the area of footprint scales as $I_{c-coils}^{0.47}$. Thus, we find two important results: 1½ degree of freedom Hamiltonian and near Hamiltonian systems respond to internal, low mode number, resonant, perturbations by reorganizing itself into large-scale coherent structure in the phase space; and further, in response to sufficiently strong external perturbation, the system again reorganizes itself into coherent phase-space structures that reflect the nature of the external perturbation. Second: In the DIII-D, the C-coils negate or neutralize the effects of the ELMs, and as a bonus, simultaneously spread the heat flux over a wider area.

An excessive concentration of heat ($\sim 15\text{-}20 \text{ MW m}^{-2}$) on the divertor plates, control of ELMS, and understanding the complex patterns of heat distribution on the plates are crucial problems in fusion science of the modern-day, large, long-pulse tokamaks. Here, we address these problems using our method of maps [1,2]. Assumption of axisymmetry in tokamaks is an idealization. Real life tokamaks are not exactly axisymmetric. By adding asymmetric magnetic perturbations, one can widen the region of heat deposition on divertor plates [1,2] and also control the ELMs. A Hamiltonian system integrated using ordinary numerical method will become non-Hamiltonian system, with completely different long-term behavior. Symplectic maps used in the method of maps are symplectic integrators that

preserve and thus respect the Hamiltonian nature of the dynamics. Here we use the symmetric simple map [3] to describe the unperturbed magnetic topology of the DIII-D upper single-null (USN) configuration in the absence of the ELMs and the C-coils. Effects of ELMs are calculated by the low m map [4], and the effects of C-coils are calculated by the dipole map [5,6]. The key parameters calculated are the width w of stochastic layer and the magnetic footprint (and its area A) as functions of the current I_{c-coil} in C-coils for the $m=1$, $n=\pm 1$ internal mode with fixed amplitude of 6×10^{-4} that is representative of its value that is expected in present-day divertor tokamaks [4].

For the shot 115467 in the DIII-D, the $q_{edge}=6.48$. In the SSM when $k=0.2623$, and $N_p=6$, $q_{edge}=6.48$, $w=0.0005$, $y_{LGS}=0.9995$, and $x_s=0.5596$. In the DIII-D, $R_{sep}=2.67$ m, $R_0=1.746$ m, and $R_{c-coil}=3.2$ m, the separation between the coil and the separatrix is $s=0.933$ m, the distance x_s between the separatrix and the magnetic axis along the x axis $x_s=0.521$ m, and $x_s/s=0.5584$. To apply the dipole map to the DIII-D, we use the same proportion in the map, and get $s=1.0021$ for the map. Since $x_{dipole}=x_s+s$, we have $x_{dipole}=0.5596+1.0021$. In DIII-D, $B_{T,0}=1.6$ T, $B_{T,sep}=1.185$ T, the effective magnetic moment M of C-coil (with $I_{c-coil}=1$ A) $=1.056$ Am², and the direction of rotation of magnetic field is counterclockwise (same as in the SSM). For the maximum current ($=20$ KA) in the C-coils, we get 52.2 Gauss for the axial dipole field at the separatrix on the x axis. In the dipole map, the amplitude of the dipole perturbation is $\delta=\delta B/B_0$. Corresponding to $\delta B_{max}=52.2$ Gauss and $B_0=1.185$ T in the DIII-D shot, the maximum value of the amplitude, δ_{max} , will be 4.4051×10^{-3} in the dipole map, and the δ will be related to the current in C-coils as $\delta=2.2025 \times 10^{-4} I_{c-coil}$ where I_{c-coil} is in KA.

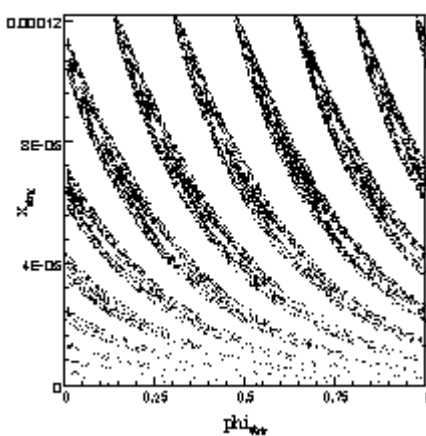
The unperturbed magnetic topology of the DIII-D in shot 115467 is represented by the SSM. The footprint is made of six toroidal strips (Fig.1). The area of the footprint, A , is 0.1361×10^{-4} . When the $m=1$, $n=\pm 1$ perturbation is turned on with $\epsilon=6 \times 10^{-4}$, the width increases to 0.01625. The magnetic topology reorganizes itself and develops a large-scale coherent structure in the phase space (Fig. 2). The area of footprint increases to 4.564×10^{-4} . Experimentally one will see this change as multiple radial heat flux peaks to a single peak, and an increase in the area of footprint by about a factor of 34. Now, we turn on the current in the C-coils. When $I_{c-coils}=0.54$ KA, the bifurcation of the footprint sets (Fig. 3), and is complete at $I_{c-coils}=1$ KA (Fig. 4). At this time, a small, new branch also begins to form in the footprint (Fig. 4). When $I_{c-coils}$ reaches 10 KA, all three branches grow to be roughly of

same shape and size (Fig. 5). On further increasing $I_{c-coils}$, this pattern continues with expanded size (Fig. 6). Width varies as $I_{c-coils}^{0.4}$ (Fig. 7). Area of footprint, A , varies as $I_{c-coils}^{0.47}$ (Fig. 8). At the maximum C-coils current of 20 KA, the area of footprint increases by about a factor of seven, while the width of chaotic layer increases by about a factor of five. When $I_{c-coils}$ is sufficiently large, the structure of footprint is reflective of the nature of external perturbation the three symmetrically placed quadrupoles.

In conclusion, $1\frac{1}{2}$ degree of freedom Hamiltonian and near Hamiltonian systems respond to internal, low mode number, resonant, perturbations by reorganizing itself into large-scale coherent structure in the phase space. In response to sufficiently strong external perturbation, the system again reorganizes itself into coherent phase-space structures that reflect the nature of the external perturbation. In the DIII-D, the C-coils negate or neutralize the effects of the ELMs, and as a bonus, simultaneously spread the heat flux over a wider area.

HA and AP than Prof. Michael Schaffer of General Atomics for valuable comments and suggestions. This work is supported by DE-FG02-01ER54624 and DE-FG02-04ER54793.

1. A. Punjabi, A. Verma, and A. Boozer, Phys. Rev. Lett. 69, 3322 (1992).
2. A. Punjabi, A. Verma, and A. Boozer, J. Plasma Phys. 52, 91 (1994).
3. A. Punjabi, H. Ali, and A. Boozer, Phys. Plasmas 4, 337 (1997).
4. H. Ali, A. Punjabi, A. Boozer, and T. Evans, Phys. Plasmas 11, 1908 (2004).
5. A. Punjabi, H. Ali, and A. Boozer, Phys. Plasmas 10, 3992 (2003).
6. H. Ali, A. Punjabi, and A. Boozer, Derivation of the dipole map, to appear in Phys. Plasmas (2004)



are
Fig. 1. Magnetic footprint when ELMs
absent and I_{c-c}

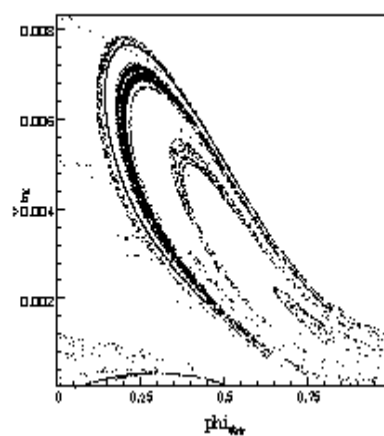


Fig. 2. Footprint when ELMs represented
by $\varepsilon=6 \times 10^{-4}$ in low mn map is turned on.

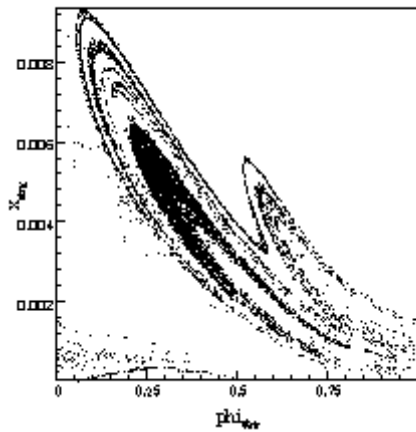


Fig. 3. Footprint when $I_{c-coils} = 0.54$ KA. Bifurcation begins.

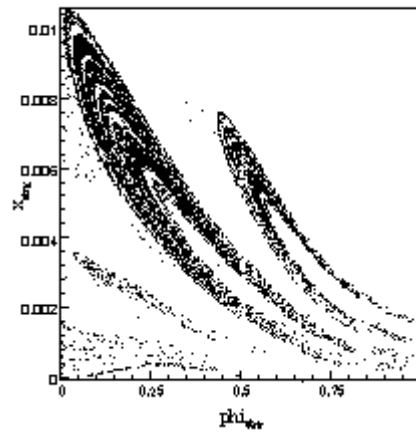


Fig. 4. Footprint when $I_{c-coils} = 1$ KA.

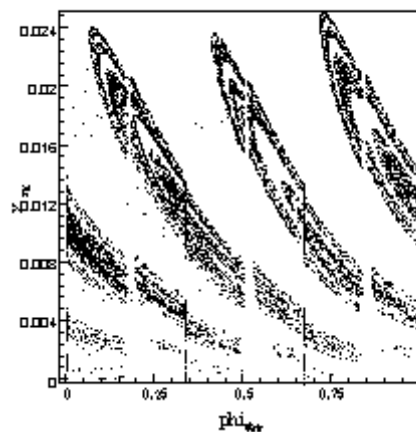


Fig. 5. Footprint when $I_{c-coils} = 10$ KA.

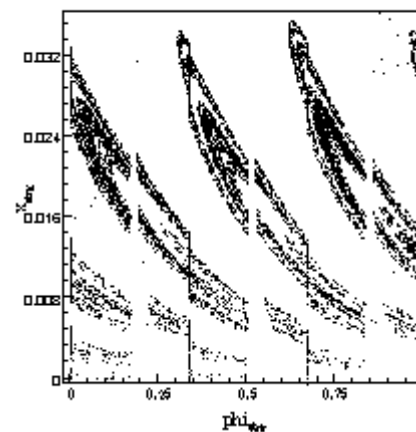


Fig. 6. Footprint when $I_{c-coils}$ is maximum, and equals to 20 KA.

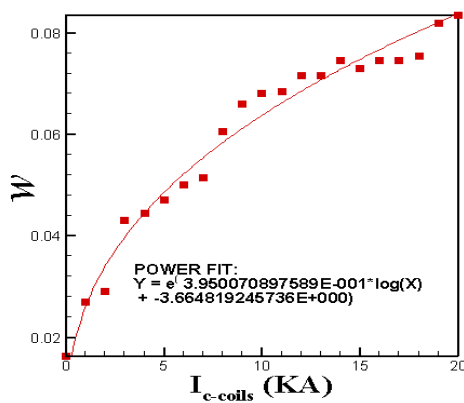


Fig. 7. Width of stochastic layer as a function of $I_{c-coils}$.

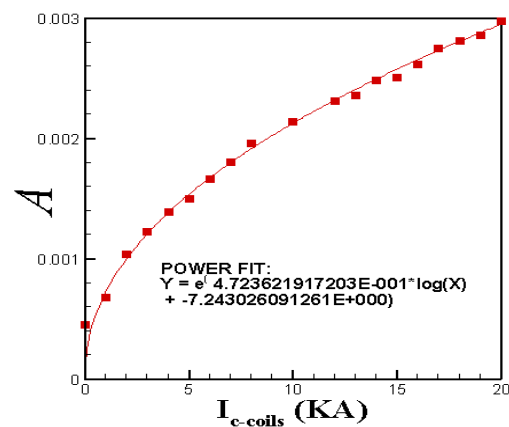


Fig. 8. Area of footprint as a function of $I_{c-coils}$.